Cardiovascular Research (2015) **106**, 478–487
doi:10.1093/cvr/cvv124

Atypical chemokine receptor 1 deficiency reduces atherogenesis in *ApoE*-knockout mice

Wuzhou Wan[1], Qian Liu[1], Michail S. Lionakis[2], Ana Paula M.P. Marino[1], Stasia A. Anderson[3], Muthulekha Swamydas[2], and Philip M. Murphy[1]*

[1]Molecular Signaling Section, Laboratory of Molecular Immunology (LMI), National Institute of Allergy and Infectious Diseases (NIAID), National Institutes of Health (NIH), Bethesda, MD, USA; [2]Fungal Pathogenesis Unit, Laboratory of Clinical Infectious Diseases, NIAID, NIH, Bethesda, MD, USA; and [3]National Heart, Lung and Blood Institute (NHLBI) Animal MRI Core, NIH, Bethesda, MD, USA

Received 15 July 2014; revised 18 March 2015; accepted 20 March 2015; online publish-ahead-of-print 9 April 2015

Time for primary review: 40 days

Aims Atypical chemokine receptor 1 (Ackr1; previously known as the Duffy antigen receptor for chemokines or Darc) is thought to regulate acute inflammatory responses in part by scavenging inflammatory CC and CXC chemokines; however, evidence for a role in chronic inflammation has been lacking. Here we investigated the role of Ackr1 in chronic inflammation, in particular in the setting of atherogenesis, using the apolipoprotein E-deficient ($ApoE^{-/-}$) mouse model.

Methods and results $Ackr1^{-/-}ApoE^{-/-}$ and $Ackr1^{+/+}ApoE^{-/-}$ littermates were obtained by crossing $ApoE^{-/-}$ mice and $Ackr1^{-/-}$ mice on a C57BL/6J background. $Ackr1^{+/+}ApoE^{-/-}$ mice fed a Western diet up-regulated Ackr1 expression in the aorta and had markedly increased atherosclerotic lesion size compared with $Ackr1^{-/-}ApoE^{-/-}$ mice. This difference was observed in both the whole aorta and the aortic root in both early and late stages of the model. Ackr1 deficiency did not affect serum cholesterol levels or macrophage, collagen or smooth muscle cell content in atherosclerotic plaques, but significantly reduced the expression of Ccl2 and Cxcl1 in the whole aorta of $ApoE^{-/-}$ mice. In addition, Ackr1 deficiency resulted in a modest decrease in T cell subset frequency and inflammatory mononuclear phagocyte content in aorta and blood in the model.

Conclusions Ackr1 deficiency appears to be protective in the *ApoE* knockout model of atherogenesis, but it is associated with only modest changes in cytokine and chemokine expression as well as T-cell subset frequency and inflammatory macrophage content.

Keywords Atherosclerosis • Inflammation • Leukocytes • Chemokine receptor

1. Introduction

Atherosclerosis, the major cause of mortality worldwide, is a chronic inflammatory disease regulated by various immune effectors, including cholesterol accumulation, pattern-recognition receptor activation, and inflammatory cell recruitment.[1,2] The activation and migration of various inflammatory cells into the vessel wall are critically regulated by chemokines and chemokine receptors, which are involved in all stages of atherosclerosis.[3] For example, chemokine receptors Ccr2, Ccr5, Ccr6, and Cx3cr1 are critical for the migration, adhesion, and survival of monocytes; Ccr1, Ccr4, Ccr5, Ccr7, Cxcr3, and Cxcr6 are required for the adhesion, recruitment, and egress of T cells; whereas neutrophils rely on Cxcr2 and Cxcr4 for their recruitment into atherosclerotic lesions.[4]

Ackr1, previously known as the Duffy antigen receptor for chemokines or Darc, is an atypical chemokine receptor in that it (i) binds highly promiscuously to both inflammatory CC and CXC chemokines, (ii) is expressed by red blood cells, endothelial cells, and cerebellar Purkinje cells, but not by leukocytes, and (iii) does not signal through G proteins.[5,6] Genome-wide association studies (GWAS) have shown that ACKR1 polymorphisms are associated with serum levels of CCL2 in both Caucasian adults and Hispanic children,[7,8] and reduced neutrophil count in African Americans.[9] These results are consistent with previous animal studies, which showed that erythrocyte Ackr1 may serve as a blood reservoir or sink to buffer plasma chemokine levels,[6,10] and endothelial cell Ackr1 can mediate chemokine transcytosis.[11] Erythrocyte ACKR1 is used by the malaria-causing protozoan *Plasmodium vivax* as a cell entry factor,[12] whereas Purkinje cell Ackr1 appears to regulate motor function and behaviour.[13]

As a regulator of inflammation, Ackr1 has been examined in various contexts, including sepsis, malaria infection, HIV, cancer, and renal

* Corresponding author. Tel: +1 301 496 8616; Fax: +1 301 402 4369, Email: pmm@nih.gov

Published by Oxford University Press on behalf of the European Society of Cardiology 2015. This work is written by (a) US Government employee(s) and is in the public domain in the US.

failure[6,10,14]; however, a role in chronic inflammatory pathologies has not yet been defined. It has been suggested that ACKR1 may have diagnostic and therapeutic implications in cardiovascular diseases since ACKR1 is expressed by erythrocytes, which are present within atherosclerotic plaques and may promote plaque growth and instability.[15] In this regard, we have investigated the role of Ackr1 in atherosclerosis in the apolipoprotein E-deficient ($ApoE^{-/-}$) mouse model.

2. Methods

2.1 Animals

$ApoE^{-/-}$ mice were purchased from Jackson Laboratories (Bar Harbor, ME, USA) and $Ackr1^{-/-}$ mice were provided by Dr Stephen C. Piper (Jefferson University School of Medicine). Both mice are on a C57BL/6J background. $Ackr1^{-/-}ApoE^{-/-}$ mice were obtained by crossing $Ackr1^{-/-}$ mice and $ApoE^{-/-}$ mice. Six-week-old female littermates were fed a high-fat Western diet (WD; TD.88137; Harlan Teklad, Madison, WI, USA) or remained on Chow diet (CD) for 10, 15, or 20 weeks as indicated. Female mice sacrificed at 16 weeks of age were subjected to all the analyses detailed below unless specified otherwise. All animal study protocols were approved by the Animal Care and Use Committee of the NIAID at the NIH (reference number: LMI8E).

2.2 Real-time quantitative PCR analysis

As previously described,[16] mouse aortas were homogenized in Trizol (Invitrogen, Carlsbad, CA, USA) and RNA was isolated using RNeasy kit (Qiagen, Valencia, CA, USA). Purified RNA was first converted into cDNA and then real-time PCR (ABI Prism 7900HT, Applied Biosystems) was used to determine the levels of total mRNA, using either SYBR Green or Taqman primers (Applied Biosystems, Carlsbad, CA, USA). All samples were normalized to GAPDH or β-actin and relative gene expression changes were determined by the $\Delta\Delta C_T$ method.

2.3 Atherosclerotic lesion analysis

The size of atherosclerotic lesions in the whole aorta and aortic root was analysed as described previously.[17] Briefly, mice were anaesthetized by intraperitoneal injection of ketamine/xylazine cocktail (ketamine, 60 mg/kg; xylazine, 8 mg/kg) and were monitored continually by assessing reflexes and respiration; cervical dislocation was used to confirm death. Mouse whole aortas and hearts were collected after perfusion, and aortas were stained with Sudan IV, while hearts were snap frozen in optimal cutting temperature compound. The frozen heart blocks were cut at 100 μm increments until the valves appeared, and then the sections were cut at 10 μm thickness. Six consecutive sections (with three leaflets of the aortic valve, 50 μm apart) were first stained with Oil Red O and then counterstained with haematoxylin (Histoserv, Inc., Germantown, MD, USA). Images of the entire aorta and aortic root were captured with Leica AF6000 LX microscope (Mannheim, Germany) and analysed by Image J (NIH) and IVision software (Biovision, Inc., Exton, PA, USA), respectively.

2.4 Magnetic resonance imaging

Animal imaging was conducted following NIH animal care and use guidelines. Magnetic resonance imaging (MRI) was performed in a 7.0 T, 16-cm horizontal Bruker MR imaging system (Bruker, Billerica, MA, USA) with Bruker ParaVision 5.0 software. Mice were anaesthetized with 2–3% isoflurane and imaged with ECG and respiratory detection using a 35 mm m2m Imaging birdcage volume coil (m2m Imaging, Cleveland, OH, USA). Magnevist (gadopentate dimeglumine, Bayer HealthCare, Montville, NJ, USA) diluted 1:10 with sterile 0.9% saline was administered IV at 0.3 mmol Gd/kg. T_1-weighted gradient echo cine images of the heart were acquired in short axis from above the base to the apex and long axis in two- and four-chamber views. Short-axis cine parameters were: repetition time TR = 10 ms, echo time TE = 3.4 ms, 11–14 frames, 30° flip angle, 2.8 × 2.8 to 3.0 × 3.0 cm field of view (FOV), 256 × 256 matrix, 1.0 mm slice thickness, 4 averages, respiratory and ECG-gated. Long-axis cine parameters differed in TR/TE (12 to14/4.4 to 4.6 ms), 8–9 frames, FOV (4.8 to 5.5 cm × 2.8 cm), matrix (512 × 256), slice thickness (0.75 mm), with 5–6 averages. MRI data were processed to determine ejection fractions, ventricular volumes, and associated functional parameters using CAAS-MRV-FARM software (Pie Medical Imaging, Netherlands).

2.5 Lipid analysis

Mouse serum samples were collected after four-hour fasting. EnzyChrom kit (BioAssay Systems, Hayward, CA, USA) and Stanbio Triglyceride LiquiColor assay kit (Stanbio Lab., Boerne, TX, USA) were used to measure the total cholesterol, HDL, LDL/VLDL, and triglyceride levels, respectively.

2.6 Immunostaining

Frozen mouse aortic root sections were stained with rat anti-mouse MOMA-2 (Serotec, Raleigh, NC; Cat#: MCA519G) and goat anti-rat Alexa Fluor 488 (Molecular Probes, Carlsbad, CA; Cat#: A-11006) for macrophages, as described previously.[16] T cells and smooth muscle cells were stained with either Alexa Fluor 488 anti-mouse CD3 antibody (BioLegend, San Diego, CA, USA; Cat#: 100210) or anti-alpha smooth muscle actin antibody [1A4] (FITC) (Abcam, Cambridge, MA, USA; Cat#: ab8211). Collagen content in the aortic root sections was determined by Masson's trichrome staining (Histoserv, Inc.). Ccl2 was stained with hamster anti-mouse Ccl2 antibody (Biolegend; Cat#:505902) and Alexa Fluor 594 conjugated goat-anti-hamster IgG (Jackson ImmunoResearch Laboratories, Inc.; Cat#: 127-585-160). For Ackr1 staining, frozen mouse aortic root sections were stained with rabbit anti-mouse Ackr1 mAb (Abcam; Cat#: ab137044) and goat anti-rabbit Alexa Fluor 488 (Abcam; Cat#: ab96895). Images were either captured by a Zeiss microscope (Jena, Germany) or a Leica DMI6000 confocal microscope (Leica Microsystems, Exton, PA, USA), and were analysed using IVision software (Biovision, Inc.) or Imaris image processing software (Bitplane USA, South Windsor, CT, USA).

2.7 ELISA assay

Mouse serum was stored at −20°C and thawed prior to ELISA measurement. Murine DuoSet ELISA Development kits (R&D Systems, Minneapolis, MN, USA) were used to determine the protein levels of Ccl2, Ccl5,Cxcl1, Il-10, and TGFβ1 (Cat#: DY479, DY478 DY453, DY417, and DY1679), according to the manufacturer's instructions.

2.8 Cell isolation and single-cell suspension

As described previously,[17] primary leucocytes were isolated from mouse whole aorta, peripheral blood, bone marrow, and spleen for further flow cytometry analysis. Briefly, mouse aortas were digested with Liberase TM and collagenase B (Roche Applied Science, Indianapolis, IN, USA; Cat#: 05401119001 and 11088807001) in RPMI at 37°C for 30 min; anti-coagulated peripheral blood was treated with lysing buffer (BD Biosciences, San Jose, CA, USA) to remove erythrocytes; bone marrow was flushed from tibia and femur with HBSS/1% FCS/10 mM HEPES; spleens were finely minced. All digested tissues and cells were passed through a 70-μm filter and washed with PBS/2 mM EDTA, and the remaining red cells were lysed with ACK lysing buffer (Quality Biological, Inc., Gaithersburg, MD, USA). Then the cells were washed three times with fluorescence activated cell sorting (FACS) buffer (PBS, 1% BSA, 0.1% sodium azide) to prepare single-cell suspensions.

2.9 *In vivo* T-cell adoptive transfer

T cells purified from $Ackr1^{+/+}ApoE^{-/-}$ and $Ackr1^{-/-}ApoE^{-/-}$ spleens by negative selection (Pan T Cell Isolation Kit, Cat#: 130-095-130; Miltenyi Biotec) were labelled with CMFDA Cell Tracker Orange or CMTMR Cell Tracker Green (Invitrogen). They were then washed with cold RPMI, resuspended in PBS, and mixed at a 1:1 ratio. 5×10^6 labelled cells were injected

intravenously into *Ackr1*$^{+/+}$*ApoE*$^{-/-}$ and *Ackr1*$^{-/-}$*ApoE*$^{-/-}$ mice, and mouse spleens were collected 18 h later for further flow cytometry analysis.

2.10 Flow cytometry

The cells were first stained with a LIVE/DEAD fluorescent dye (Invitrogen; Cat#: L-23105) for 15 min (1:1000) at room temperature and blocked with rat anti-mouse CD16/32 for 15 min (1:200) at 4°C. According to the manufacturer's instructions, the cells were then stained 30 min at 4°C with the following mouse-specific fluorochrome-conjugated antibodies: CD45-PE (eBioscience, Cat#: 12-0451-83), CD3-FITC (BD Biosciences, Cat#: 555274), CD3-APC (BioLegend, Cat#: 100312), CD4-APC-Cy7 (eBioscience, Cat#: 47-0042-82), CD8-PE-Cy7 (eBioscience, Cat#: 25-0081-82), CD11c-APC (eBioscience, Cat#: 17-0114-82), MHCII-Pacific Blue (BioLegend, Cat#: 116422), CD19-PerCP-Cy5.5 (BioLegend, Cat#: 115534), CD11b-PerCP-Cy5.5 (BD Biosciences, Cat#: 550993),

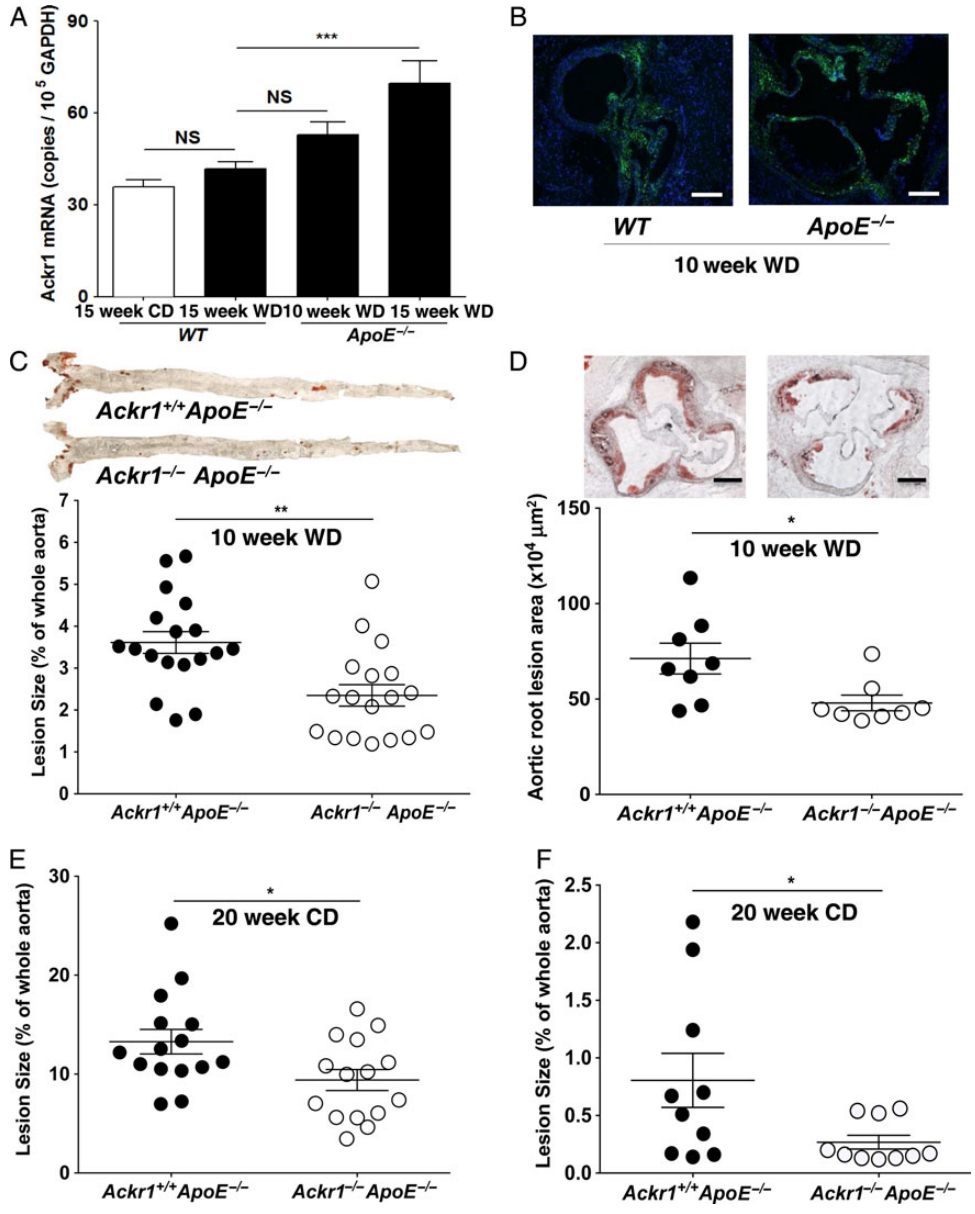

Figure 1 Ackr1 is expressed in mouse aortic samples and its deficiency reduces atherogenesis in *ApoE*$^{-/-}$ mice. (*A*) Real-time PCR analysis of Ackr1 expression in the whole aorta of wild-type C57BL/6J mice and *ApoE*$^{-/-}$ mice that had been on a CD or WD for 10 or 15 weeks ($n = 4$ mice per group; $^*P = 0.024$, $^{**}P = 0.001$; NS, $P > 0.05$). All samples were normalized to GAPDH. (*B*) Representative IHC staining pictures of Ackr1 (green) and DAPI (blue) on frozen aortic root sections from wild type C57BL/6J mice (left) and *ApoE*$^{-/-}$ mice (right) that had been on a WD for 10 weeks ($n = 3$ mice per group, 10 weeks on WD; bar = 250 µm). (*C*) Upper part: representative photographs of Sudan IV-stained mouse whole aorta of *Ackr1*$^{+/+}$*ApoE*$^{-/-}$mice and *Ackr1*$^{-/-}$*ApoE*$^{-/-}$ mice; lower part: quantification of the atherosclerotic lesion size is shown as percentage of the whole aorta ($n = 18$ mice per group, 10 weeks on WD; $^{**}P = 0.001$). (*D*) Upper part: representative photographs of frozen aortic root sections stained with Oil Red O; lower part: quantification of the staining for aortic root lesion size, shown as mean areas ($n = 8$ mice per group, 10 weeks on WD; $^*P < 0.05$; Bar = 250 µm). (*E* and *F*) Quantification of atherosclerotic lesion size in the whole aorta of *Ackr1*$^{+/+}$*ApoE*$^{-/-}$ mice and *Ackr1*$^{-/-}$*ApoE*$^{-/-}$ mice that had been fed either a WD (*E*) or a CD (*F*) for 20 weeks ($n = 10$–15 mice per group, $^*P < 0.05$).

Ly6C-FITC (BD Biosciences, Cat#: 553942), Ly6G-APC-Cy7 (BD Biosciences, Cat#: 560600), 7/4-Alexa Fluor 647 (AbD Serotec., Cat#: MCA771A647), NK1.1-APC (eBioscience, Cat#: 17-5941-82), F4/80-PE-Cy7 (eBioscience, Cat#: 25-4801-82), Annexin V-APC (BD Biosciences, Cat#: 550475), Propidium iodide staining solution (BD Biosciences, Cat#: 556547), Ki67-PE (BioLegend, Cat#: 652404). Flow cytometry was performed on a BD LSRII flow cytometer (BD Biosciences) and data were analysed with FlowJo software (version 9.4.2; Treestar, Ashland, OR, USA).

2.11 Bone marrow-derived macrophages

Mice were sacrificed by cervical dislocation and bone marrow was flushed from tibia and femur with PBS and 2 mM EDTA, and then cultured in RPMI1640 with 40 ng/mL macrophage colony stimulating factor to obtain bone marrow-derived macrophages (BMDM). BMDM were stimulated with either 25 ng/mL IFNγ and 100 ng/mL lipopolysaccharide (LPS) or 10 ng/mL IL-4 to induce M1 and M2 macrophages, respectively.

2.12 Statistical analysis

All data were presented as the mean ± SEM and analysed using either unpaired parametric *t* tests (two-tailed) or ANOVA analysis with Prism 6 (GraphPad Software). Bonferroni correction was performed where it is appropriate, and the cut-off for statistical significance was $P < 0.05$ (****$P < 0.0001$; ***$P < 0.001$; **$P < 0.01$; *$P < 0.05$; NS, $P \geq 0.05$).

3. Results

3.1 Ackr1 deficiency reduces atherogenesis in *ApoE*$^{-/-}$ mice

Ackr1 mRNA was present in the whole aorta of both wild-type and *ApoE*$^{-/-}$ C57BL/6 mice, as shown by qPCR analysis (*Figure 1A*). Its expression was significantly increased in *ApoE*$^{-/-}$ mice fed a WD for 15 weeks compared with control wild-type mice fed a WD for 15 weeks (*Figure 1A*). Also, Ackr1 protein was identified in the aortic root

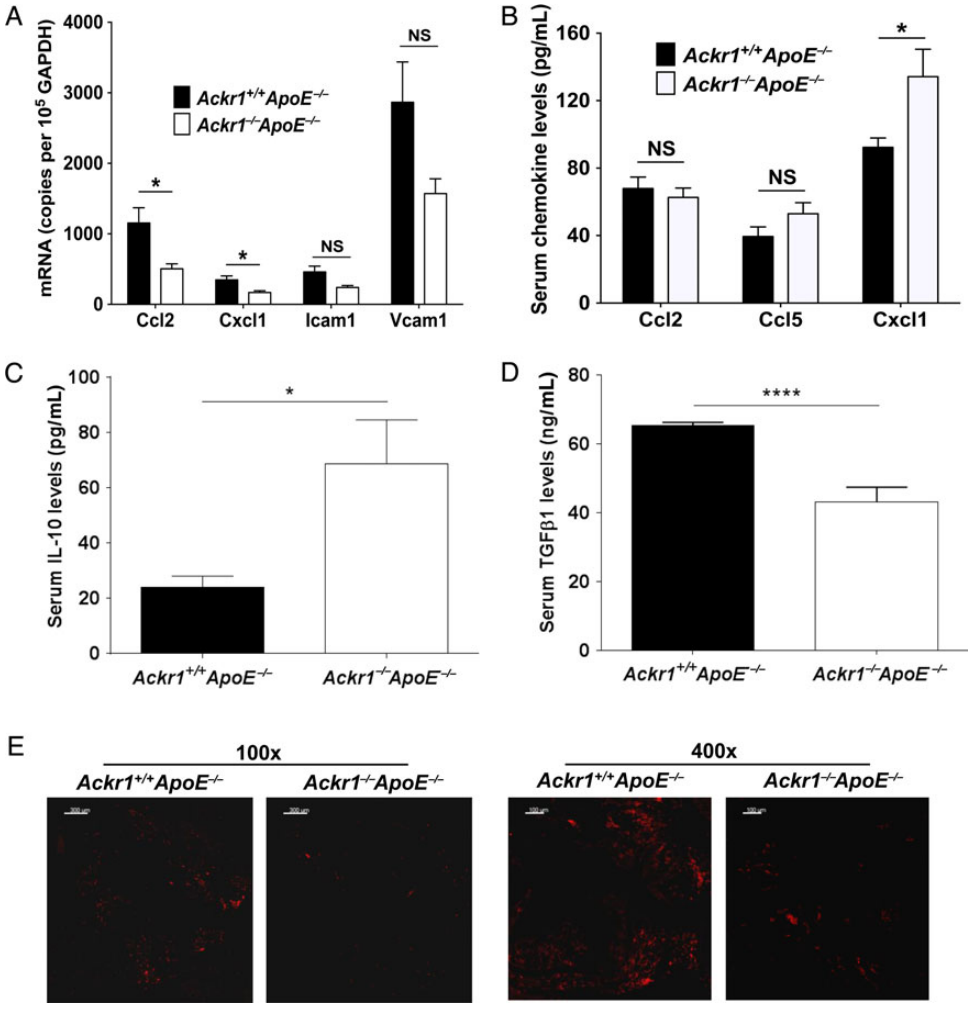

Figure 2 Ackr1 deficiency changes the aortic expression of certain cytokines and adhesion molecules. (*A*) Real-time PCR analysis of the expression of Ccl2, Cxcl1, Icam1, and Vcam1 from *Ackr1*$^{+/+}$*ApoE*$^{-/-}$ mice and *Ackr1*$^{-/-}$*ApoE*$^{-/-}$ mice ($n = 8–10$ mice per group, 10 weeks on WD; * $P < 0.05$). (*B*) ELISA analysis of the serum levels of Ccl2, Ccl5, and Cxcl1 in *Ackr1*$^{+/+}$*ApoE*$^{-/-}$ mice and *Ackr1*$^{-/-}$*ApoE*$^{-/-}$ mice ($n = 9–20$ mice per group, 10 weeks on WD; NS, $P > 0.05$; * $P < 0.05$). (*C* and *D*) ELISA analysis of the serum levels of Il-10 (*C*), and TGFβ1 (*D*) in *Ackr1*$^{+/+}$*ApoE*$^{-/-}$ mice and *Ackr1*$^{-/-}$*ApoE*$^{-/-}$ mice ($n = 15–17$ mice per group, 10 weeks on WD; * $P < 0.05$, **** $P < 0.0001$). (*E*) Representative IHC images of Ccl2 in the aortic root sections from *Ackr1*$^{+/+}$*ApoE*$^{-/-}$ mice and *Ackr1*$^{-/-}$*ApoE*$^{-/-}$ mice ($n = 3$ mice per group, 10 weeks on WD; bar = 300 μm for the 100× images and bar = 100 μm for the 400× images).

samples by IF staining (*Figure 1B*). In order to directly examine the role of Ackr1 in atherogenesis, *Ackr1*$^{-/-}$*ApoE*$^{-/-}$ and *Ackr1*$^{+/+}$ *ApoE*$^{-/-}$littermates were generated by crossing *Ackr1*$^{-/-}$ mice and *ApoE*$^{-/-}$ mice. We found that after 10 weeks on a WD, *Ackr1*$^{-/-}$ *ApoE*$^{-/-}$ mice had ~35% lower atherosclerotic lesion size in the whole aorta than *Ackr1*$^{+/+}$*ApoE*$^{-/-}$ mice (*Figure 1C*, lower panel).

Table I Ackr1 deficiency does not affect lipid profiles in the *ApoE*$^{-/-}$ mouse model of atherosclerosis

Genotype	Total cholesterol	HDL cholesterol	LDL/VLDL cholesterol	Triglyceride
Ackr1$^{+/+}$*ApoE*$^{-/-}$	977 ± 41	68 ± 14	826 ± 38	177 ± 6
Ackr1$^{-/-}$*ApoE*$^{-/-}$	879 ± 69	86 ± 18	751 ± 48	199 ± 11

Female *Ackr1*$^{+/+}$*ApoE*$^{-/-}$ mice and *Ackr1*$^{-/-}$*ApoE*$^{-/-}$ mice ($n = 9–18$ mice per group) were 16 weeks old and had been on a WD for 10 weeks at the time of euthanasia. Data are the mean ± SEM and lipid values are in mg/dL.

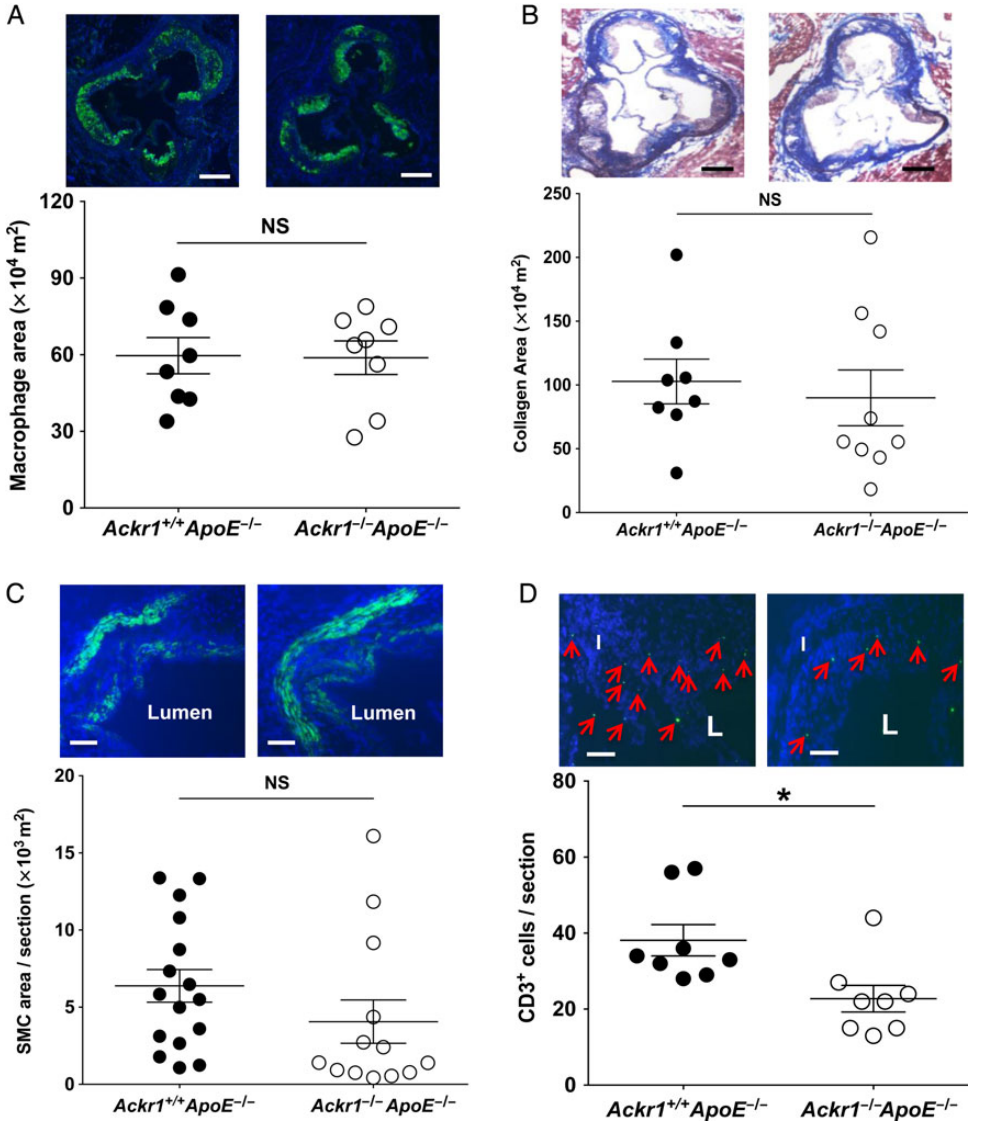

Figure 3 Ackr1 deficiency reduces T-cell accumulation in the aortic root of *ApoE*$^{-/-}$ mice. (*A–D*) Upper part: representative photographs of frozen aortic root sections stained with MOMA-2 for macrophages (*A*), Masson's Trichrome for collagen (*B*), α smooth muscle actin for SMCs (*C*), and CD3 for T cells (*D*) (L indicates lumen and I indicates intima; arrows indicate CD3$^+$ cells); lower part: quantification of the staining for macrophages (*A*), collagen (*B*), SMCs (*C*) and T cells (*D*), shown as either mean areas or numbers ($n = 8$ mice per group, 10 weeks on WD; *$P < 0.05$; NS, $P > 0.05$). Bar = 250 μm in (*A*) and (*B*) and bar = 50 μm in (*C*) and (*D*).

Nevertheless, the lesion patterns were similar in both control and knockout mice, with most of the lesions found at the lesser curvature of the aortic arch (*Figure 1C*, upper panel). Atherosclerotic lesion size in the aortic root sections of *Ackr1*$^{-/-}$*ApoE*$^{-/-}$ mice was also significantly reduced by about 33% compared with *Ackr1*$^{+/+}$*ApoE*$^{-/-}$ mice (*Figure 1D*). The reduction in lesion size compared with control mice persisted in *Ackr1*$^{-/-}$*ApoE*$^{-/-}$ mice fed a WD for 20 weeks (*Figure 1E*). Also, atherosclerotic lesion size was significantly reduced in aortas from *Ackr1*$^{-/-}$*ApoE*$^{-/-}$ mice fed a CD for 20 weeks (*Figure 1F*), indicating that Ackr1 affects both early and late stages of atherogenesis. MRI demonstrated that the stroke volume and cardiac output of *Ackr1*$^{-/-}$*ApoE*$^{-/-}$ mice were both significantly increased compared with *Ackr1*$^{+/+}$*ApoE*$^{-/-}$ mice, but the cardiac dimensions were similar (see Supplementary material online, *Table S1*), suggesting that Ackr1 deficiency may result in an increased adrenergic drive.

3.2 Ackr1 deficiency reduces the aortic expression of chemokines and adhesion molecules in *ApoE*$^{-/-}$ mice

It is known that Ackr1 can bind to a variety of inflammatory CC and CXC chemokines,[5,6] so here we first examined the effect of Ackr1 deficiency on the expression of all known chemokines, chemokine receptors and some adhesion molecules, inflammatory cytokines in the whole aorta by qPCR analysis. The levels of Ccl2 and Cxcl1 were significantly reduced in *Ackr1*$^{-/-}$*ApoE*$^{-/-}$ mice compared with *Ackr1*$^{+/+}$*ApoE*$^{-/-}$ mice, whereas most other factors tested were not affected (*Figure 2A* and Supplementary material online, *Figure S1*). Surprisingly, the serum levels of Ccl2 and Ccl5 were not affected by Ackr1 deficiency, but the level of Cxcl1 was significantly increased in *Ackr1*$^{-/-}$*ApoE*$^{-/-}$ mice (*Figure 2B*). At the same time, the serum level of Il-10 was significantly increased but the level of TGFβ1 was reduced in *Ackr1*$^{-/-}$*ApoE*$^{-/-}$ mice (*Figure 2C* and *D*). The protein expression of Ccl2 in the aortic root plaque was determined by immunohistochemical staining, and in agreement with the RNA data *Ackr1*$^{-/-}$*ApoE*$^{-/-}$ mice expressed much less Ccl2 protein than the *Ackr1*$^{+/+}$*ApoE*$^{-/-}$ mice (*Figure 2E*).

3.3 Ackr1 deficiency and T-cell accumulation in atherosclerotic lesions of *ApoE*$^{-/-}$ mice

Both cholesterol accumulation and inflammatory cell recruitment can affect atherosclerotic lesion development.[1] However, the serum levels of total cholesterol, HDL, LDL/VLDL and triglycerides between age- and diet-matched *Ackr1*$^{-/-}$*ApoE*$^{-/-}$ mice and *Ackr1*$^{+/+}$*ApoE*$^{-/-}$ mice were similar (*Table 1*). Both the absolute content and the percentages of macrophages, collagen and smooth muscle cells in the aortic root sections of these mice were also similar (*Figure 3A–C* and data not shown). The total number of CD3$^+$ T cells per histological section was greater in *Ackr1*$^{+/+}$*ApoE*$^{-/-}$ mice than in *Ackr1*$^{-/-}$*ApoE*$^{-/-}$ mice (*Figure 3D*); however, the difference was similar in magnitude to the difference in plaque size in these mice. The content of CD4$^+$ T cells assessed by flow cytometry in both the whole aorta and blood was significantly reduced in *Ackr1*$^{-/-}$*ApoE*$^{-/-}$ mice compared with *Ackr1*$^{+/+}$*ApoE*$^{-/-}$ controls (*Figure 4A* and *B*). There was also a reduction in CD8$^+$ T cells in the spleen of *Ackr1*$^{-/-}$*ApoE*$^{-/-}$ mice, but no difference was found for bone

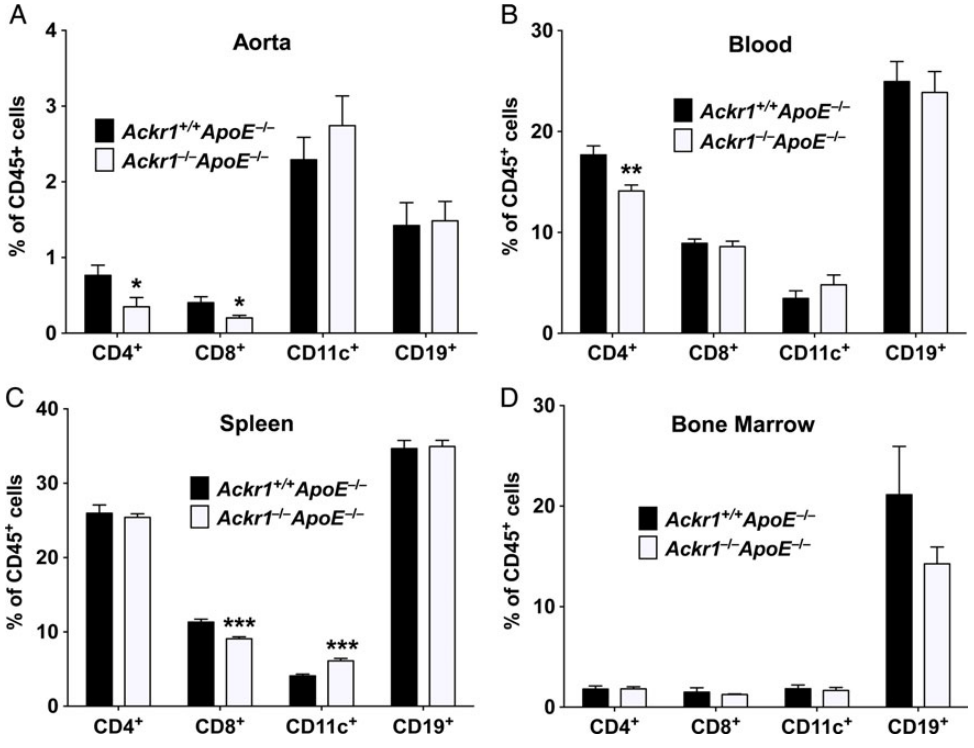

Figure 4 Ackr1 deficiency skews T-cell subset frequency in the whole aorta and blood of *ApoE*$^{-/-}$ mice. (*A–D*) Percentages of CD4$^+$, CD8$^+$ T cells, CD11c$^+$MHCII$^+$ DCs and CD19$^+$ B cells in the whole aorta (*A*), circulating blood (*B*), spleen (*C*), and bone marrow (*D*) of *Ackr1*$^{+/+}$*ApoE*$^{-/-}$ mice and *Ackr1*$^{-/-}$*ApoE*$^{-/-}$ mice were determined by FACS analysis ($n = 7–10$ mice per group, 10 weeks on WD) (For aorta CD4$^+$ $^*P = 0.033$, CD8$^+$ $^*P = 0.022$; for blood CD4$^+$ $^{**}P = 0.004$; for spleen CD8$^+$ $^{***}P = 0.0004$, CD11c$^+$ $^{***}P = 0.0001$).

marrow (*Figure 4C* and *D*). This reduction was not caused by apoptosis or proliferation since flow cytometry data showed that Ackr1 deficiency did not affect the level of apoptosis or proliferation of T cells (see Supplementary material online, *Figure S2A* and *B*). Instead, T-cell adoptive transfer experiments with splenocytes suggested that *Ackr1*$^{-/-}$*ApoE*$^{-/-}$ recipient mice had less T-cell migration into the spleen compared with *Ackr1*$^{+/+}$*ApoE*$^{-/-}$ recipient mice, whereas the donor genotype had no effect on the migration ability of T cells (*Figure 5A–C*), suggesting that the reduced aortic total T-cell accumulation in *Ackr1*$^{-/-}$*ApoE*$^{-/-}$ mice may be caused by impaired T-cell recruitment.

3.4 Ackr1 deficiency skews monocytes/macrophages towards a less inflammatory state in *ApoE*$^{-/-}$ mice

Monocytes are involved in both the initiation and progression of atherosclerosis, and macrophages are the most abundant cell type identified in atherosclerotic lesions[2]; therefore, we next assessed the effect of Ackr1 deficiency on monocytes and macrophages. Although the content of Ly6C^{hi}, Ly6C^{low} and total monocytes in the aorta, blood, bone marrow, and spleen of *Ackr1*$^{-/-}$*ApoE*$^{-/-}$ mice and *Ackr1* $^{+/+}$*ApoE*$^{-/-}$ mice were similar (*Figure 6A*, *B* and Supplementary material online, Figure 3*A–D*), the ratio of Ly6C^{hi} monocytes to Ly6C^{low} monocytes in the whole aorta and blood of *Ackr1*$^{-/-}$*ApoE*$^{-/-}$ mice was slightly reduced (*Figure 6C* and *D*). The apoptosis or proliferation of Ly6C^{hi}, Ly6C^{low} monocytes and Ly6G^{+} neutrophils was not affected by Ackr1 deficiency in *ApoE*$^{-/-}$ mice (see Supplementary material online, *Figure S2A* and *B*). Further analyses with BMDM showed that macrophages from *Ackr1*$^{-/-}$*ApoE*$^{-/-}$ mice expressed fewer M1 markers (e.g. Il-1β) but more M2 markers (e.g. Fizz1) even before differentiation (*Figure 6E*), consistent with an attenuated inflammatory phenotype. After differentiation (LPS/IFNγ stimulation, or IL-4 stimulation *ex vivo*), the expression of M1 markers like Il-12β and iNOS were significantly reduced for macrophages from *Ackr1*$^{-/-}$*ApoE*$^{-/-}$ mice (*Figure 6F*),

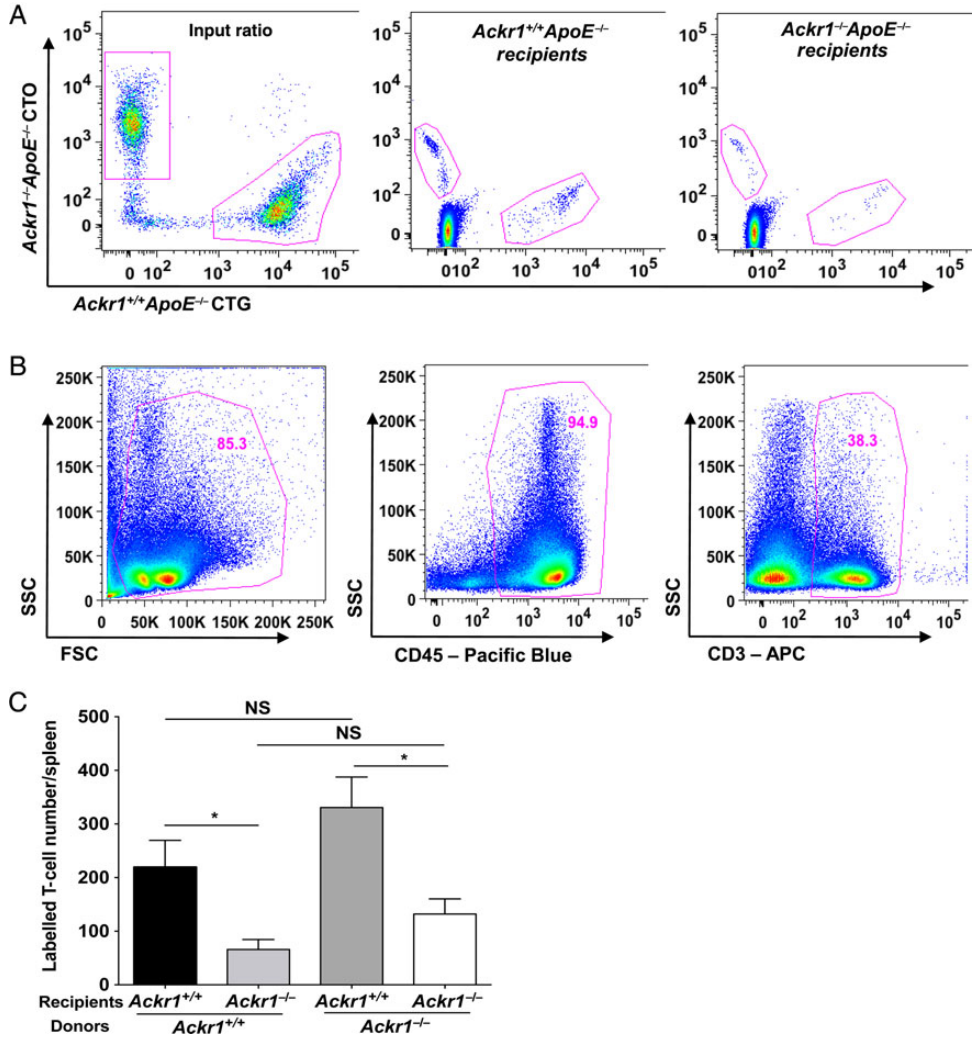

Figure 5 Ackr1 deficiency reduces T cell trafficking in *ApoE*$^{-/-}$ mice. (*A*) Representative flow cytometry staining of *Ackr1*$^{+/+}$*ApoE*$^{-/-}$ and *Ackr1*$^{-/-}$*ApoE*$^{-/-}$ T cells labelled with cell tracker green (CTG) and cell tracker orange (CTO), both before (left) and 18 h after the adoptive transfer (middle and right). (*B*) Representative flow cytometry staining for CD3^{+} T cells after the adoptive transfer. Spleen cells were first gated by forward scatter, side scatter, and then were gated by their expression of CD45 and CD3. (*C*) The number of labelled T cells in the recipient *Ackr1*$^{+/+}$*ApoE*$^{-/-}$ mice and *Ackr1*$^{-/-}$*ApoE*$^{-/-}$ mice were determined by flow cytometry, and 2.5 × 10^{5} spleen cells were collected for the analysis ($n = 3$ mice per group, 10 weeks on WD, * $P < 0.05$; experiment was repeated twice).

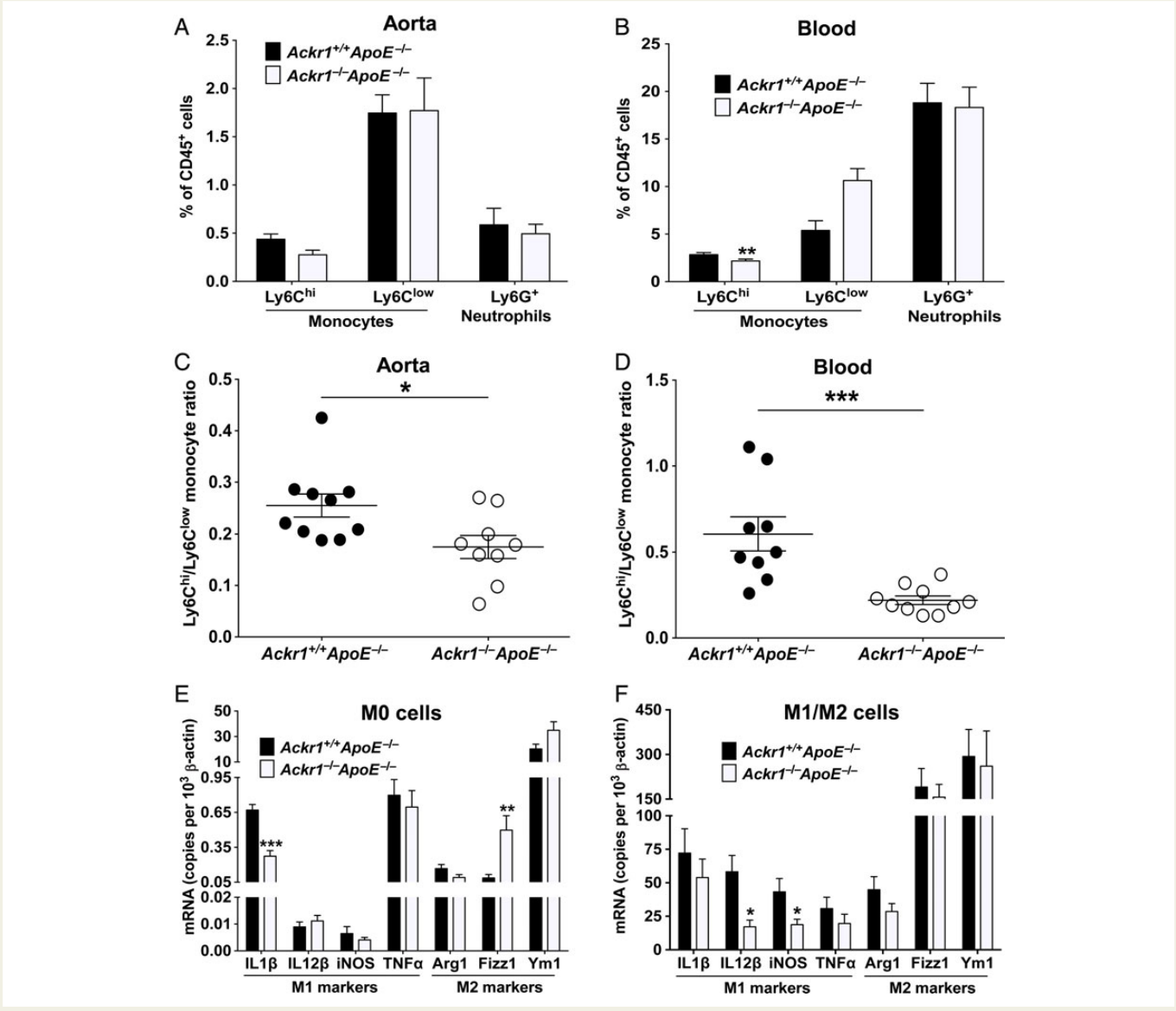

Figure 6 Ackr1 deficiency skews monocytes/macrophages towards a less inflammatory state in $ApoE^{-/-}$ mice. Percentages of $Ly6C^{hi}$ and $Ly6C^{low}$ monocytes in the whole aorta (*A*) and circulating blood (*B*) of $Ackr1^{+/+}ApoE^{-/-}$ mice and $Ackr1^{-/-}ApoE^{-/-}$ mice were determined by FACS analysis and the ratio of $Ly6C^{hi}/Ly6C^{low}$ monocytes was shown correspondingly in (*C*) and (*D*) ($n = 9–10$ mice per group, 10 weeks on WD; $^{*}P = 0.0231$, $^{**}P = 0.0014$, $^{***}P = 0.0009$). (*E* and *F*) BMDM from $Ackr1^{+/+}ApoE^{-/-}$ mice and $Ackr1^{-/-}ApoE^{-/-}$ mice were stimulated with either 25 ng/mL IFNγ and 100 ng/mL LPS or 10 ng/mL IL-4 to derive M1/M2 macrophages. Real-time PCR was used to analyse the mRNA levels of IL-1β, IL-12β, iNOS, TNFα (M1 markers) and Arg1, Fizz1, Ym1 (M2 markers) before (*E*) and after (*F*) stimulation. All samples were normalized to β-actin ($n = 4–7$ mice per group; $^{***}P = 0.0005$, $^{**}P = 0.005$, $^{*}P < 0.05$).

suggesting that Ackr1 deficiency may skew BMDM differentiation towards a less inflammatory state.

4. Discussion

Ackr1 is an atypical chemokine receptor that binds promiscuously to various inflammatory CC and CXC chemokines, including CCL2, CCL5, CCL17, CXCL1, CXCL5, and CXCL8, without signalling through G proteins.[18,19] Acting through typical G protein-coupled chemokine receptors, Ackr1 ligands can induce activation and migration of many leucocyte subsets, including monocytes, T cells, and neutrophils into the vessel wall, and play a pathogenic role during atherosclerosis development.[4] For example, genetic deletion of Ccl2, Ccl17, and Cxcl1 all significantly reduce atherosclerotic lesion size in corresponding atherosclerosis mouse models.[20–22] Since Ackr1 may mediate transcytosis and scavenging of inflammatory chemokines,[6] it is important to know whether it may directly affect atherogenesis.

Previous studies have mainly focused on the role of Ackr1 in acute inflammation, such as in malaria infection,[12] LPS challenge,[23,24] and acute renal failure.[25] ACKR1 absence from the red blood cell surface of West Africans confers resistance to *Plasmodium vivax* infection[12]; Ackr1-deficient mice have been reported to have increased inflammatory responses to LPS challenge,[23] but to be protected from acute renal failure.[25] Here we demonstrate that genetic deletion of Ackr1 in

ApoE$^{-/-}$ mice impairs atherosclerosis development at both early and late stages, indicating that Ackr1 may also play a critical role in chronic inflammation. Genetic deletion of the G protein-coupled chemokine receptors Ccr2, Ccr5, and Ccr6 in the *ApoE*$^{-/-}$ mouse model has been reported to reduce atherosclerotic lesion size by 36, 40, and 50%, respectively,[16] similar to the magnitude of protection afforded by Ackr1 knockout (35%).

Human *ACKR1* polymorphisms are associated with serum CCL2 levels in Caucasians (e.g. the Asp42Gly variant was associated with higher levels of CCL2)[7,8] and *Ackr1*$^{-/-}$ mice have been shown to have lower plasma concentrations of Ccl2.[26] However, Ackr1 deficiency did not affect serum levels of Ccl2 in the *ApoE*$^{-/-}$ mouse model. Instead, serum concentrations of Cxcl1 were significantly increased. There was a marked reduction of both Ccl2 and Cxcl1 expression in the whole aorta and aortic root of *Ackr1*$^{-/-}$*ApoE*$^{-/-}$ mice. Increased serum Cxcl1 levels in Ackr1 knockouts may be due to the loss of Ackr1's chemokine transcytosis function, in this case from the serum into aorta, consistent with current models of how Ackr1 regulates chemokine distribution between blood and tissue during inflammation.[6,10] Cxcl1 is known to be chemotactic for neutrophils,[4] but very few neutrophils were found in plaque in the model by immunohistochemical staining (data not shown).

Ackr1 deficiency in *ApoE*$^{-/-}$ mice did not affect cholesterol levels, plaque stability, or macrophage accumulation in the lesions. Instead, Ackr1 deficiency reduced the total aorta content of T cells, possibly by regulating the expression of relevant inflammatory chemokines on endothelial cells. This is consistent with the ability of Ackr1 to mediate chemokine transcytosis and the finding that Ackr1 overexpression on mouse blood vessel endothelium-enhanced leucocyte extravasation.[11,27] However, whether reduced total T-cell content is a causal factor in reducing plaque size in Ackr1 knockout mice or instead is secondary to decreased plaque size remains to be determined.

Ackr1 deficiency also appeared to skew monocytes and macrophages into a less inflammatory state. A direct mechanism on macrophages involving signalling by chemokines whose expression is regulated by Ackr1 has not previously been reported. However, indirect mechanisms could also be involved. For example, Ackr1 modulation of chemokine levels could affect the balance of Th1/Th2 CD4^{+} T cells and their signature cytokines in lesions. The maintenance of M2 macrophages is thought to require IL-4-producing Th2 cells and the switch from M2 to M1 macrophages may be triggered by a Th1 environment.[28,29] Lower levels of Ccl2 and higher levels of Il-10 in atherosclerotic lesions of *Ackr1*$^{-/-}$*ApoE*$^{-/-}$ mice may bias the content of infiltrating macrophages towards M2.

To summarize, here we provide the first evidence that Ackr1 plays a critical role in chronic inflammation, in particular in the *ApoE*$^{-/-}$ mouse model of atherogenesis. The mechanism may involve control of cytokine and chemokine balance in blood and plaque, including regulation of the important T cell and macrophage-targeted chemokine Ccl2. Taken together, our data suggest that Ackr1 may be considered as a potential target for therapeutic development in atherosclerosis.

Supplementary material

Supplementary material is available at *Cardiovascular Research* online.

Acknowledgements

We thank Dr Stephen C. Peiper for providing the *Ackr1*$^{-/-}$ mice, Dr Hongwei Zhang for the technical help with BD LSRII flow cytometer, Dr Sundar Ganesan for the technical help with Leica DMI6000 confocal microscope and Steven Nelson Bradford for performing animal anaesthesia and related animal preparation for MRI.

Conflict of interest: none declared.

Funding

This work was supported by the Division of Intramural Research of the National Institute of Allergy and Infectious Diseases at the National Institutes of Health.

References

1. Libby P, Lichtman AH, Hansson GK. Immune effector mechanisms implicated in atherosclerosis: from mice to humans. *Immunity* 2013;**38**:1092–1104.
2. Galkina E, Ley K. Immune and inflammatory mechanisms of atherosclerosis. *Annu Rev Immunol* 2009;**27**:165–197.
3. Koenen RR, Weber C. Chemokines: established and novel targets in atherosclerosis. *EMBO Mol Med* 2011;**3**:713–725.
4. Wan W, Murphy PM. Regulation of atherogenesis by chemokines and chemokine receptors. *Arch Immunol Ther Exp (Warsz)* 2013;**61**:1–14.
5. Bachelerie F, Ben-Baruch A, Burkhardt AM, Combadiere C, Farber JM, Graham GJ, Horuk R, Sparre-Ulrich AH, Locati M, Luster AD, Mantovani A, Matsushima K, Murphy PM, Nibbs R, Nomiyama H, Power CA, Proudfoot AE, Rosenkilde MM, Rot A, Sozzani S, Thelen M, Yoshie O, Zlotnik A. International Union of Pharmacology. LXXXIX. Update on the extended family of chemokine receptors and introducing a new nomenclature for atypical chemokine receptors. *Pharmacol Rev* 2014;**66**:1–79.
6. Nibbs R, Graham GJ. Immune regulation by the atypical chemokine receptors. *Nat Rev Immunol* 2013;**13**:815–829.
7. Schnabel RB, Baumert J, Barbalic M, Dupuis J, Ellinor PT, Durda P, Dehghan A, Bis JC, Illig T, Morrison AC, Jenny NS, Keaney JF Jr, Gieger C, Tilley C, Yamamoto JF, Khuseyinova N, Heiss G, Doyle M, Blankenberg S, Herder C, Walston JD, Zhu Y, Vasan RS, Klopp N, Boerwinkle E, Larson MG, Psaty BM, Peters A, Ballantyne CM, Witteman JC, Hoogeveen RC, Benjamin EJ, Koenig W, Tracy RP. Duffy antigen receptor for chemokines (Darc) polymorphism regulates circulating concentrations of monocyte chemoattractant protein-1 and other inflammatory mediators. *Blood* 2010;**115**:5289–5299.
8. Voruganti VS, Laston S, Haack K, Mehta NR, Smith CW, Cole SA, Butte NF, Comuzzie AG. Genome-wide association replicates the association of Duffy antigen receptor for chemokines (DARC) polymorphisms with serum monocyte chemoattractant protein-1 (MCP-1) levels in Hispanic children. *Cytokine* 2012;**60**:634–638.
9. Reich D, Nalls MA, Kao WH, Akylbekova EL, Tandon A, Patterson N, Mullikin J, Hsueh WC, Cheng CY, Coresh J, Boerwinkle E, Li M, Waliszewska A, Neubauer J, Li R, Leak TS, Ekunwe L, Files JC, Hardy CL, Zmuda JM, Taylor HA, Ziv E, Harris TB, Wilson JG. Reduced neutrophil count in people of African descent is due to a regulatory variant in the Duffy antigen receptor for chemokines gene. *PLoS Genet* 2009;**5**:e1000360.
10. Novitzky-Basso I, Rot A. Duffy antigen receptor for chemokines and its involvement in patterning and control of inflammatory chemokines. *Front Immunol* 2012;**3**:266.
11. Pruenster M, Mudde L, Bombosi P, Dimitrova S, Zsak M, Middleton J, Richmond A, Graham GJ, Segerer S, Nibbs RJ, Rot A. The Duffy antigen receptor for chemokines transports chemokines and supports their promigratory activity. *Nat Immunol* 2009;**10**:101–108.
12. Zimmerman PA, Ferreira MU, Howes RE, Mercereau-Puijalon O. Red blood cell polymorphism and susceptibility to Plasmodium vivax. *Adv Parasitol* 2013;**81**:27–76.
13. Schneider EH, Fowler SC, Lionakis MS, Swamydas M, Holmes G, Diaz V, Munasinghe J, Peiper SC, Gao JL, Murphy PM. Regulation of Motor Function and Behavior by Atypical Chemokine Receptor 1. *Behav Genet* 2014;**44**:498–515.
14. Horne K, Woolley IJ. Shedding light on DARC: the role of the Duffy antigen/receptor for chemokines in inflammation, infection and malignancy. *Inflamm Res* 2009;**58**:431–435.
15. Apostolakis S, Chalikias GK, Tziakas DN, Konstantinides S. Erythrocyte Duffy antigen receptor for chemokines (DARC): diagnostic and therapeutic implications in atherosclerotic cardiovascular disease. *Acta Pharmacol Sin* 2011;**32**:417–424.
16. Wan W, Lim JK, Lionakis MS, Rivollier A, McDermott DH, Kelsall BL, Farber JM, Murphy PM. Genetic Deletion of Chemokine Receptor Ccr6 Decreases Atherogenesis in ApoE-Deficient Mice. *Circ Res* 2011;**109**:374–381.
17. Wan W, Lionakis MS, Liu Q, Roffê E, Murphy PM. Genetic deletion of chemokine receptor Ccr7 exacerbates atherogenesis in ApoE-deficient mice. *Cardiovasc Res* 2013;**97**:580–588.
18. Szabo MC, Soo KS, Zlotnik A, Schall TJ. Chemokine class differences in binding to the Duffy antigen-erythrocyte chemokine receptor. *J Biol Chem* 1995;**270**:25348–25351.

19. Kashiwazaki M, Tanaka T, Kanda H, Ebisuno Y, Izawa D, Fukuma N, Akimitsu N, Sekimizu K, Monden M, Miyasaka M. A high endothelial venule-expressing promiscuous chemokine receptor DARC can bind inflammatory, but not lymphoid, chemokines and is dispensable for lymphocyte homing under physiological conditions. *Int Immunol* 2003;**15**: 1219–1227.
20. Gu L, Okada Y, Clinton SK, Gerard C, Sukhova GK, Libby P, Rollins BJ. Absence of monocyte chemoattractant protein-1 reduces atherosclerosis in low density lipoprotein receptor-deficient mice. *Mol Cell* 1998;**2**:275–2581.
21. Weber C, Meiler S, Döring Y, Koch M, Drechsler M, Megens RT, Rowinska Z, Bidzhekov K, Fecher C, Ribechini E, van Zandvoort MA, Binder CJ, Jelinek I, Hristov M, Boon L, Jung S, Korn T, Lutz MB, Förster I, Zenke M, Hieronymus T, Junt T, Zernecke A. CCL17-expressing dendritic cells drive atherosclerosis by restraining regulatory T cell homeostasis in mice. *J Clin Invest* 2011;**121**:2898–2910.
22. Boisvert WA, Santiago R, Curtiss LK, Terkeltaub RA. A leukocyte homologue of the IL-8 receptor CXCR-2 mediates the accumulation of macrophages in atherosclerotic lesions of LDL receptor-deficient mice. *J Clin Invest* 1998;**101**:353–363.
23. Dawson TC, Lentsch AB, Wang Z, Cowhig JE, Rot A, Maeda N, Peiper SC. Exaggerated response to endotoxin in mice lacking the Duffy antigen/receptor for chemokines (DARC). *Blood* 2000;**96**:1681–1684.
24. Luo H, Chaudhuri A, Zbrzezna V, He Y, Pogo AO. Deletion of the murine Duffy gene (Dfy) reveals that the Duffy receptor is functionally redundant. *Mol Cell Biol* 2000;**20**: 3097–3101. Erratum in: *Mol Cell Biol* 2003;23:3030.
25. Zarbock A, Schmolke M, Bockhorn SG, Scharte M, Buschmann K, Ley K, Singbartl K. The Duffy antigen receptor for chemokines in acute renal failure: A facilitator of renal chemokine presentation. *Crit Care Med* 2007;**35**:2156–2163.
26. Fukuma N, Akimitsu N, Hamamoto H, Kusuhara H, Sugiyama Y, Sekimizu K. A role of the Duffy antigen for the maintenance of plasma chemokine concentrations. *Biochem Biophys Res Commun* 2003;**303**:137–139.
27. Lee JS, Frevert CW, Wurfel MM, Peiper SC, Wong VA, Ballman KK, Ruzinski JT, Rhim JS, Martin TR, Goodman RB. Duffy antigen facilitates movement of chemokine across the endothelium in vitro and promotes neutrophil transmigration in vitro and in vivo. *J Immunol* 2003;**170**:5244–5251.
28. Khallou-Laschet J, Varthaman A, Fornasa G, Compain C, Gaston AT, Clement M, Dussiot M, Levillain O, Graff-Dubois S, Nicoletti A, Caligiuri G. Macrophage plasticity in experimental atherosclerosis. *PLoS One* 2010;**5**:e8852.
29. Loke P, Gallagher I, Nair MG, Zang X, Brombacher F, Mohrs M, Allison JP, Allen JE. Alternative activation is an innate response to injury that requires CD4+ T cells to be sustained during chronic infection. *J Immunol* 2007;**179**:3926–3936.